Journal of Applied Mechanics and Technical Physics, Vol. 50, No. 6, pp. 1063–1070, 2009

PROPAGATION OF A LOW-FREQUENCY WAVE COMPONENT IN A MODEL OF A BLOCK MEDIUM

V. A. Saraikin

UDC 539.3

This paper studies the properties of a model of a block medium consisting of absolutely rigid blocks separated by deformable layers. The model is proposed to describe the low-frequency spectral region of a perturbation wave propagating in the medium of this structure. The model is based on the assumption that the low-frequency part of the wave train provides the least distorted information on the average characteristics of the structure of the medium on the wave pathway. Calculation of waves in a one-dimensional assembly of blocks (rods) and deformable layers show that the model ignoring the deformation of the blocks is applicable only in the case where the stiffness of the layer is low compared to the stiffness of the rod. A correction is applied to eliminate this restriction in the case of a long-wave approximation.

Key words: *block medium, conditions on contact layers, nonstationary waves, crumpling, stiffness of spring.*

The need to take into account the discrete structure of a real rock massif was noted in [1, 2]. The discrete structure of the material at various scale levels was taken into account in the solution of problems of dynamic crack propagation in [3, 4]. A two-dimensional model for the dynamics of a discrete medium consisting of rigid rectangular blocks in contact through thin elastic layers was examined in [5]. It was assumed that layers between the blocks consisted of two parts, each of which was a surface layer of a block weakened by defects and hence loaded to a greater degree than the core of the block. Therefore, it was assumed in [5] that the kernel is absolutely rigid. Because inertia was ignored, the approximate consideration of the deformation of thin compound layers was actually reduced to their replacement by equivalent springs in both tension-compression and shear. Later, the possibility of crumpling of roughness uniformly distributed on the layer contact surface was taken into account with the use of Hertz theory [6–8].

We study the specificity of wave propagation in a block medium using a one-dimensional model. An assembly consisting of n rectangular blocks (below, rods of length $2H$) separated by thin layers of length $2h$ consisting of two identical parts is examined. The last rod of the assembly rests against an absolutely rigid wall. The entire assembly was initially statically compressed to eliminate tensile stresses and, hence, the possible loss of contacts during dynamic loading of the left end of the assembly. Therefore, all quantities to be calculated below should be understood as deviations from the given initial state; in other words, a tensile stress not exceeding the initial compression is admitted in the propagating waves.

We will seek a numerical solution under the assumption that both the rods and layers are deformed elastically. A characteristic element of this chain is shown in Fig. 1a, where rectangles correspond to rods between which there is a spring layer. In this case, at the point of connection of the springs, the displacements of their ends are set equal to each other: $v^- = v^+$. The longitudinal displacement $u^k(t, x)$ in the kth rod is described by the wave equation

Institute of Mining, Siberian Division, Russian Academy of Sciences, Novosibirsk 630091. Novosibirsk State University, Novosibirsk 630090; vsaraikin@gmail.com. Translated from Prikladnaya Mekhanika i Tekhnicheskaya Fizika, Vol. 50, No. 6, pp. 177–185, November–December, 2009. Original article submitted December 19, 2008.

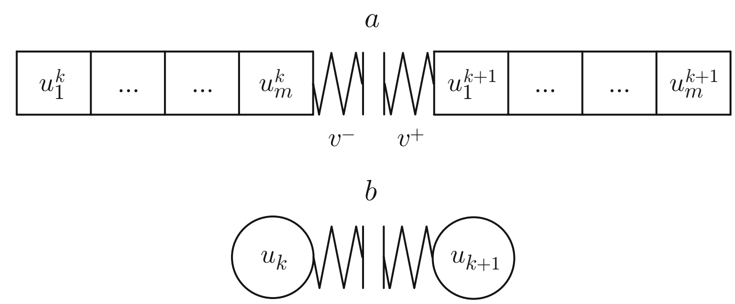

Fig. 1. Element of the block structure with deformable rod (a) and rigid rod (b).

$$\frac{\partial^2 u^k}{\partial x^2} = \frac{1}{v_b^2}\,\ddot{u}^k, \qquad v_b = \sqrt{\frac{E}{\rho}},$$
$$(2H+2h)(k-1) \leqslant x \leqslant (2H+2h)k - 2h \qquad (k = 1, 2, \ldots, n). \tag{1}$$

Here E and ρ are the Young modulus and the density of the rod material, respectively; the dots denote time derivatives; the x axis is directed from left to right.

We assume that the springs have viscosity; therefore, taking into account the linear relationship of stress to strain and strain rate in the form

$$\sigma = E_s(\varepsilon + \eta\dot{\varepsilon})$$

we write the strain relation for the springs as

$$\sigma = c_s(u_r^{k+1} - u_l^k) + c_s\eta(\dot{u}_r^{k+1} - \dot{u}_l^k) \qquad (k = 1, 2, \ldots, n-1). \tag{2}$$

Here $c_s = E_s/(2h)$ is the reduced total stiffness of the springs of one compound layer (the stiffness per unit area), E_s is the Young modulus of the layer material, and η is a viscosity parameter; the subscripts l and r correspond to the displacements at the left and right ends of the rods; the superscript is the rod number.

Let us formulate boundary conditions. The left end of the first rod is subjected to the compressing dynamic load:

$$\sigma^1(t, 0) = E\,\frac{\partial u_l^1}{\partial x} = f(t) \leqslant 0, \tag{3}$$

at the sites of contact between the rods and the spring, we impose the condition of equality of the stresses

$$\sigma_r^k = \sigma_l^{k+1} = c_s(u_l^{k+1} - u_r^k) + c_s\eta(\dot{u}_r^{k+1} - \dot{u}_l^k) \qquad (k = 1, 2, \ldots, n-1), \tag{4}$$

and at the right end of the assembly, the condition of equality of the displacement to zero:

$$u_r^n = 0.$$

The initial conditions of the problem are zero.

The problem was solved by the finite difference method. Each rod was divided into m parts with a step $2dx$. In the calculation of the displacements $u_l^k = u_1^k, u_2^k, \ldots, u_{m-1}^k, u_m^k = u_r^k$ in the kth rod and $u_l^{k+1} = u_1^{k+1}, u_2^{k+1}, \ldots, u_{m-1}^{k+1}, u_m^{k+1} = u_r^{k+1}$ in the $(k+1)$th rod, the wave equation (1) at the end point of the kth rod and at the initial point of the $(k+1)$th rod was written in discrete form with the conjugation conditions (4) taken into account:

$$\ddot{u}_m^k = \frac{c_s}{2\rho\,dx}\,[u_1^{k+1} - u_m^k + \eta(\dot{u}_1^{k+1} - \dot{u}_m^k)] - \frac{c_{dx}}{2\rho\,dx}\,(u_m^k - u_{m-1}^k),$$
$$\ddot{u}_1^{k+1} = \frac{c_{dx}}{2\rho\,dx}\,(u_2^{k+1} - u_1^{k+1}) - \frac{c_s}{2\rho\,dx}\,[u_1^{k+1} - u_m^k + \eta(\dot{u}_1^{k+1} - \dot{u}_m^k)] \tag{5}$$
$$c_{dx} = E/(2\,dx) \qquad (k = 1, 2, \ldots, n-1).$$

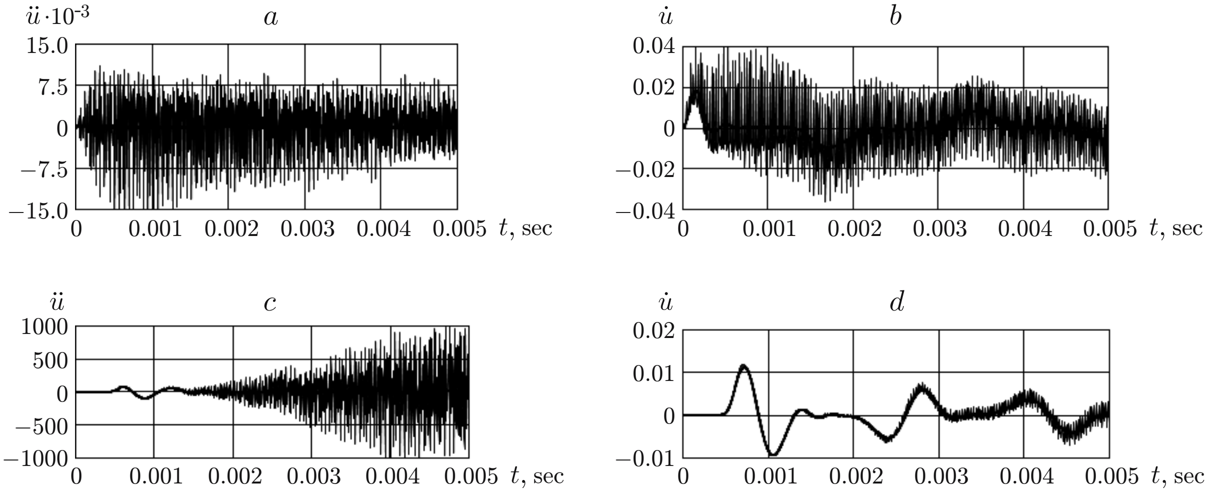

Fig. 2. Oscillograms of accelerations (a and c) and velocities (b and d) for the second rod of the assembly (a and b) and eighth rod of the assembly (c and d) at $E = 1.922 \cdot 10^4$ MPa, $2H = 0.085$ m, $E_s = 20$ MPa, $2h = 0.001$ m, $t_0 = 5 \cdot 10^{-6}$ sec, and $\eta = 0.00001$ sec: thin curves correspond to the numerical solution of the problem in the exact formulation and thick curves correspond to the solution in the long-wave approximation (6).

The boundary condition (3) is written in finite differences in a standard way. After time discretization of (5) with a step τ, we obtained an explicit computation cross type scheme.

Along with the exact equations (1)–(5), we considered a model of the medium in which the rods were considered rigid and were replaced by point masses (Fig. 1b). In this case, we have n masses which interact through a compound spring ($v^- = v^+$). Then,

$$m_1 \ddot u_1 = c_s(u_2 - u_1) + c_s\eta(\dot u_2 - \dot u_1) - f(t),$$

$$m_k \ddot u_k = c_s(u_{k+1} - 2u_k + u_{k-1}) + c_s\eta(\dot u_{k+1} - 2\dot u_k + \dot u_{k-1}), \tag{6}$$

$$m_k = 2H\rho = \text{const} \qquad (k = 2, 3, \ldots, n-1).$$

Similar problems were considered in [9, 10]. In the present paper, we give more complete calculation results with the irreversible crumpling of the layers on the contact boundary taken into account.

In the calculation of problems (1)–(6), the material characteristics corresponded to brick (in rods) and rubber (in layers) [9]: $\rho = 2000$ kg/m^3, $v_b = 3100$ km/sec, $E = 1.922 \cdot 10^4$ MPa, and $E_s = 20$ MPa. The linear dimensions of the elements in the assembly had the following values: $2H = 0.085$ m and $2h = 0.001$ m. It was assumed that the loading curve had a pulsed dome-like shape with a maximum at the point t_0:

$$f(t) = \begin{cases} p(t^2/t_0^2 - 2t/t_0)^2, & 0 \leqslant t \leqslant 2t_0, \\ 0, & t > 2t_0. \end{cases}$$

The value of the loading at the maximum point was set equal to $p = -1$ MPa.

Each rod was divided into 25 parts. In all calculations, the time step had a fixed small value $\tau = 10^{-9}$ sec (the period of wave reflections in the rod was $5.48 \cdot 10^{-5}$ sec to keep the high frequencies due to a change in the solution because of repeated wave reflections in the rods. The viscosity parameter of the springs was set equal to $\eta = 10^{-5}$ sec.

Figures 2a and 3a shows acceleration oscillograms on the segment $0 \leqslant t \leqslant 0.005$ sec, and Figs. 2b and 3b show their corresponding velocity oscillograms.

Figure 2 corresponds to the case $n = 10$, $t_0 = 5 \cdot 10^{-6}$ sec. Figures 2a and 2b show the development of the wave process at the center of the second rod (in the exact problem) and on the second mass, and Fig. 2c and d show the variations of the quantities at the center of the eighth rod and on the eighth mass. High-frequency oscillations

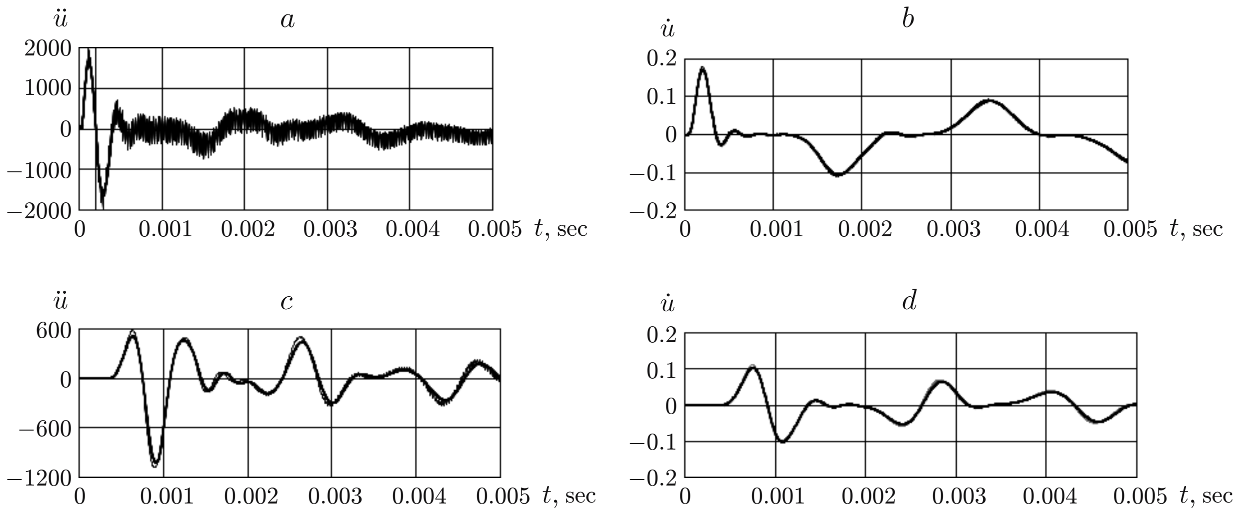

Fig. 3. Oscillograms of accelerations (a and c) and velocities (b and d) at $E = 1.922 \cdot 10^4$ MPa, $2H = 0.085$ m, $E_s = 20$ MPa, $2h = 0.001$ m, $t_0 = 5 \cdot 10^{-5}$ sec, and $\eta = 0.000\,01$ sec (notation the same as in Fig. 2).

are not a calculation error for the difference scheme used. Each curve in Fig. 2 was constructed by 1000 points chosen from $5 \cdot 10^6$ calculated values; i.e., between each two points there are 5000 points. By considerably scaling up the time axis in Fig. 2, one can see that oscillations arise under repeated reflections inside the rods. The curves shown in Fig. 2 qualitatively describe the variation of the high frequencies of the exact solution. It is evident that, according to approximation (6), high-frequency waves do not propagate over the assembly, the amplitude of accelerations of the low-frequency part is insignificant (two orders of magnitude smaller than that in the high-frequency part of the perturbation spectrum), i.e., in the model with masses, high frequencies are filtered out. We note that if the accelerations of low-frequency waves are scaled up in the oscillograms, one can see that the maxima and minima in it correspond to oscillations in the high-frequency part of the spectrum (see Fig. 2c and d). After the loading wave arrives at the second rod near the unloaded boundary of the assembly, the rod begins to vibrate (see Fig. 2a). In the eighth rod, velocity oscillations during unloading develop later; in this rod, the effect of the viscosity of the layers manifests itself as the distance traveled by the wave increases.

Figure 3 corresponds to the case $n = 10$, $t_0 = 5 \cdot 10^{-5}$ sec, i.e., compared to the case examined above, the loading duration — the time of action of the load is ten times larger, and the duration is approximately equal to the period of oscillations of the rod. With this loading duration, the velocity values in the exact and approximate solutions are almost identical, i.e., the low-frequency approximation is in good agreement with the exact solution. This may be due to the fact that low frequencies make a major contribution to the propagating perturbations. According to the exact solution, observed acceleration oscillations arise in the second rod at the moment when the wave comes from the unloaded end.

In all examined cases, the displacement curves are almost identical and the stresses vary in the same manner as the velocities in Fig. 2b and d and Fig. 3b and d.

The further increase in the loading duration improves the agreement of the solutions t_0.

Calculations were performed for an assembly with more rigid layers. With all other parameters constant, the Young modulus was increased by a factor of 100: $E_s = 2 \cdot 10^3$ MPa. The calculations show that, in this case, the solution given by Eqs. (6), differs from the exact solution: for the approximate model, the perturbation propagation velocity is considerably higher, and the amplitudes differ significantly. The differences increased with increasing stiffness of the layers.

The difference between the solutions is due the neglect of the stiffness of the rods during their replacement by point masses. It turns out that, if the rod mass is assumed to be concentrated at a point, the elastic work done in the rod cannot be ignored. For the replacement to be on the average equivalent, the point mass should done work the same way as a spring sequentially attached to a layer with the reduced stiffness of the rod $c_b = E/(2H)$.

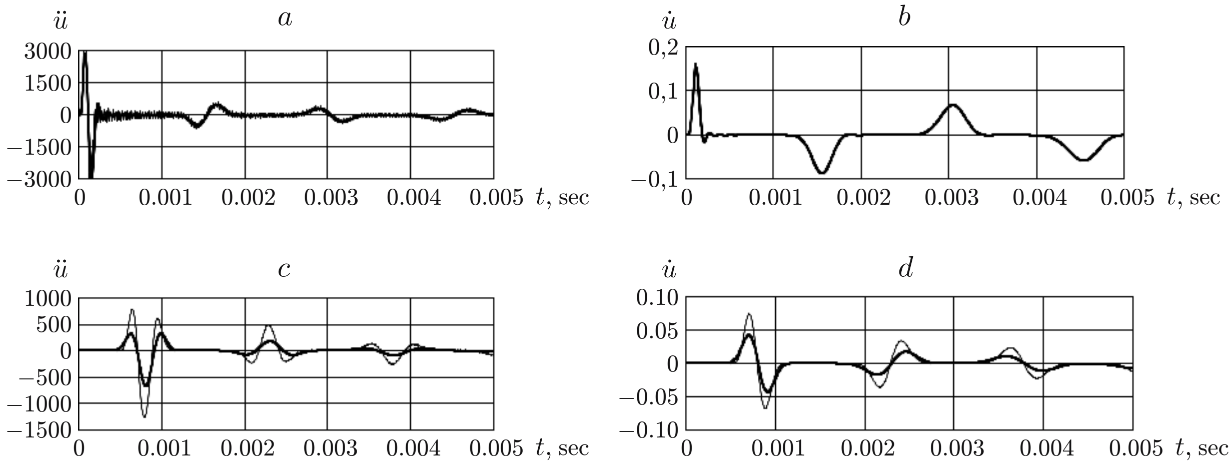

Fig. 4. Oscillograms of accelerations (a and c) and velocities (b and d) for second rod (second mass) of the assembly (a and b) and eighteenth rod (eighteenth mass) of the assembly (c and d) at $E_s = 2 \cdot 10^3$ MPa, $2h = 0.01$ m, $t_0 = 5 \cdot 10^{-5}$ sec, and $n = 20$: thin curves correspond to the numerical solution of the problem in the exact formulation and thick curves correspond to the solution in the long-wave approximation (6).

In this case, for the same contact area between the cross section of the rod and the layer, the total elongation of the block and layer and the loads that arise in them should satisfy the equalities

$$x_b + x_s = x,$$

$$c_b x_b = c_s(x_s + \eta \dot{x}_s) = c_{sb}(x + \eta_{sb} * \dot{x}).$$

Here the asterisk denotes convolution in time and x is the distance between the centers of neighboring masses.

The function $\eta_{sb}(t)$ and convolution are required to describe the time development of the effect of the rod strain on the viscous process in the layer. Using Laplace transform in time with the parameter s, we obtain the system for the images

$$x_b^L + x_s^L = x^L,$$

$$c_b x_s^L = c_s(1 + \eta s)x_s^L = c_{sb}(1 + \eta_{sb} s)x^L,$$

and, solving it for the image of the required load, we have

$$\sigma^L = c_{sb}(1 + \eta_{sb} s)x^L = \frac{c_s c_b}{c_b + c_s}\Big(1 + \frac{c_b}{c_s}\,\frac{s}{s + a/\eta}\Big)x^L.$$

From this, converting to the originals, we obtain

$$\sigma = c_{sb}(x + \eta_{sb} * \dot{x}), \qquad \eta_{sb} = (c_b/c_s)\,\mathrm{e}^{-at/\eta}, \qquad a = 1 + c_b/c_s,$$

where the coefficient before the parenthesis indicates that the reduced stiffness of the characteristic cell in the chain of masses and springs is equal to

$$c_{sb} = \frac{c_s}{1 + c_s/c_b} = \frac{c_s}{1 + E_s H/(Eh)}. \tag{7}$$

Hence, in relations (2)–(6), the stiffness of the spring c_s should be replaced by the stiffness c_{sb} (7) equal to the effective stiffness of the cell in the rod layer system, and in the case of the presence of viscosity, the corresponding terms should be replaced by convolutions.

The calculations were performed for the following values of the parameters: $E_s = 2 \cdot 10^3$ MPa, $2h = 0.01$ m, $t_0 = 5 \cdot 10^{-5}$ sec, and $n = 20$. The remaining parameters were not changed.

Time dependences of the accelerations and velocities are shown in Fig. 4. It is evident that the exact and approximate solutions differ only slightly. The greatest difference is observed at the extremum points. In the calculations performed for even more rigid springs, the exact and approximate solutions are also in good agreement.

From (7), it follows that the model consisting of rigid blocks can be used if the stiffnesses of the elements of the structure satisfy the condition

$$E_s/h \ll E/H.$$

In the case of absolutely rigid masses ($c_b \to \infty$), the viscous component in the convolution in the limit becomes a concentrated delta function:

$$\eta_{sb} = (c_b/c_s)\,\mathrm{e}^{-at/\eta} \to \eta\delta(t).$$

After the corresponding replacement in (2)–(6), we obtain system (6).

It was assumed above that two springs which are a layer work as a unit, i.e., at the site of their connection, the equality $v^- = v^+$ holds. We will assume that between the springs there is an additional element (between the vertical lines in Fig. 1); then, $v^- \neq v^+$. As such an element we consider roughness on the contact boundary between the layers which has average height $R \ll h$. The roughness can be crumpled, which is taken into account according to Hertz theory. We calculate the stiffness of such series-connected springs. Let C be the total stiffness that corresponds to the decrease in the length y as the sum of the decrease in the lengths of three elements:

$$y_1 = v^- - u_k, \qquad y_2 = v^+ - v^-, \qquad y_3 = u_{k+1} - v^+.$$

From this it follows that

$$y = u_{k+1} - u_k = 2h\varepsilon$$

(ε is the representation of the strain in discrete form).

The forces acting on each spring are identical, and, hence,

$$\sigma = Cy = 2c_s y_1 = c_c(y_2)y_2 = 2c_s y_3 \tag{8}$$

[$c_c(y_2)$ is the nonlinear stiffness which depends on the magnitude of crumpling and $c_c(y_2)y_2$ is the contact stress].

Assuming that the roughnesses are semicircles of radius R, according to Hertz theory we have [8]

$$c_c = c_s r\sqrt{-\varepsilon}, \qquad \varepsilon = \frac{u_{k+1} - u_k}{2h} \leqslant 0, \quad r = \left(\frac{h}{aR}\right)^{3/2}, \quad y_2 \approx 2\varepsilon,$$

where a is a dimensionless constant.

Relation (8) leads to the expression

$$\frac{1}{C} = \frac{1}{2c_s} + \frac{1}{c_c} + \frac{1}{2c_s},$$

which corresponds to three series-connected springs; therefore, the stiffness of the compound layer is equal to

$$C = \frac{c_c}{1 + c_c/c_s} = \frac{c_s r\sqrt{-\varepsilon}}{1 + r\sqrt{-\varepsilon}}. \tag{9}$$

From relation (9), it follows that, as the strain increases considerably, the compound spring in the compression limit begins to behave as a linear spring with stiffness c_s.

Finally, taking into account the stiffness of the rod, we represent the stiffness $c(\varepsilon)$ of a characteristic element of the assembly consisting of a rod, two springs, and the material in the zone of nonlinear crumpling:

$$c(\varepsilon) = \frac{c_s r\sqrt{-\varepsilon}}{1 + r(1 + E_s H/(Eh))\sqrt{-\varepsilon}}, \qquad \varepsilon \leqslant 0.$$

To take into account the effect of roughness on the contact boundary in the compound layer, this stiffness value should be substituted for c_s in expressions (4)–(6).

Assuming that the crumpling on the contact boundary is irreversible, the stresses acting on the mass (in the exact formulation, on the rods) from the layers should be calculated by the formula

$$\sigma = \begin{cases} c(\varepsilon)\varepsilon, & \varepsilon \leqslant \varepsilon_0 < 0, \\ c_{sb}(\varepsilon - \varepsilon_0) + c(\varepsilon_0)\varepsilon_0, & \varepsilon_0 < \varepsilon. \end{cases} \tag{10}$$

Here $\varepsilon_0 < 0$ is the strain under compression. If the compression increases, the motion on the diagram $\sigma - \varepsilon$ occurs along the nonlinear branch (Fig. 5), and if the compression decreases, the unloading and repeated loading occur

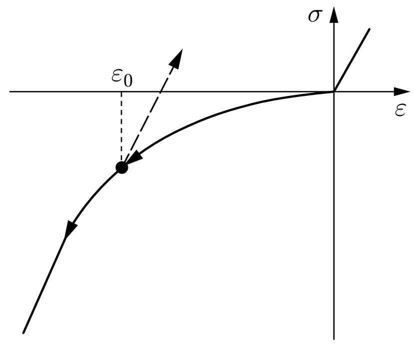

Fig. 5. The σ–ε diagram of an element of the structure for irreversible crumpling of roughness on the contact boundary inside the compound layer: the dashed curve shows the unloading site.

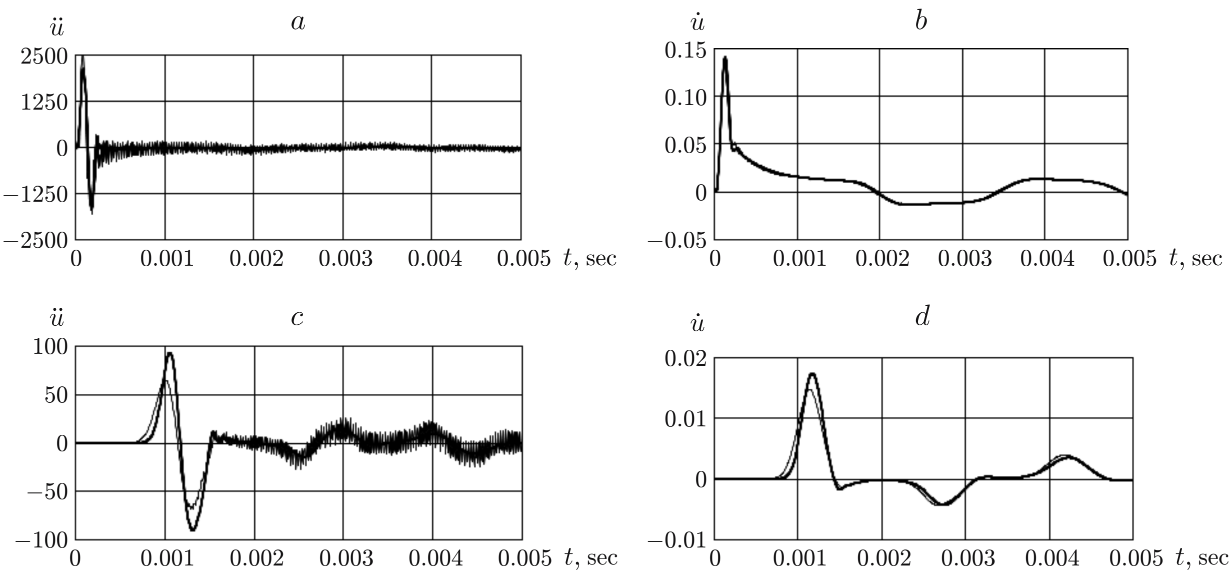

Fig. 6. Acceleration (a and c) and velocity (b and d) oscillograms for $E_s = 2 \cdot 10^3$ MPa, $2h = 0.01$ m, $t_0 = 5 \cdot 10^{-5}$ sec, $n = 20$, $R = 0.2h$, and $a = 1$ (notation the same as in Fig. 4).

along the linear region (dashed curve) until the strain during repeated compression exceeds the value ε_0 reached before unloading.

The dependence of the coefficients in the equation of state on the characteristics of the structure is similar to the dependence occurring for composite materials if their effective moduli are calculated through the corresponding characteristics of the components and the sizes of the characteristic cell by the rule of mixtures.

Calculations (see Fig. 4) were also performed taking into account the presence of the zone of contact with irreversible crumpling of roughness [see (10)] for the following parameter values: $E_s = 2 \cdot 10^3$ MPa, $R = 0.2h$, $2h = 0.01$ m, $t_0 = 5 \cdot 10^{-5}$ sec, $a = 1$, and $n = 20$.

The time dependences of accelerations and velocities are given in Fig. 6 for the same elements of the assembly as in Fig. 4. The variations in accelerations and velocities determined by the exact and approximate solutions are similar to those in Fig. 4. The largest differences are also observed at the points of local extrema. In the presence of crumpling, the element of the layer becomes less rigid, resulting in an increase in the oscillations of the rod in the unloading wave. In addition, irreversible crumpling leads to a decrease in the amplitude maxima of the calculated quantities compared to the amplitude maxima in Fig. 4, this difference increasing with increasing distance traveled by the wave.

Accounting for the crumpling of roughness on the contact boundary is meaningful for layers of sufficiently great thickness. Thus, the calculations performed with and without accounting for roughness for an assembly in which the layer thickness is 10 times smaller ($2h = 0.001$) did not reveal a large difference between the solutions.

The study performed allow the following conclusion to be drawn: for a block medium with a complex shape, it is possible to construct a three-dimensional model of propagation of low-frequency oscillations. In this case, the exact shape of the blocks is apparently not so important if the longitudinal and shear stiffnesses of the blocks in the normal and shear direction are correctly specified on the contact boundaries of the blocks, i.e., the main elastic properties and linear dimensions that determine the stiffness of the blocks in these directions.

This work was supported by the Russian Foundation for Basic Research (Grant Nos. 06-05-64738 and 06-05-64596) and Council on Grants of the President of the Russian Federation for Support of Leading Scientific Schools (Grant NSh-3803.2008.5).

REFERENCES

1. M. A. Sadovskii, "Natural humpiness of rock," *Dokl. Akad. Nauk SSSR*, **247**, No. 4, 829–831 (1979).
2. M. V. Kurlenya, V. N. Oparin, and V. I. Vostrikov, "Formation of elastic wave trains during pulsed excitation of block media: Waves of the pendulum type V_μ," *Dokl. Akad. Nauk SSSR*, **333**, No. 4, 515–521 (1993).
3. L. I. Slepyan and Sh. A. Kulakhmetova, "Crack propagation in a mass consisting of rigid blocks with elastic layers," *Izv. Akad. Nauk SSSR, Fiz. Zemli*, No. 12, 17–23 (1986).
4. L. I. Slepyan, *Models and Phenomena in Fracture Mechanics*, Springer-Verlag, Berlin–Heidelberg (2002).
5. V. A. Saraikin, M. V. Stepanenko, and O. V. Tsareva, "Elastic waves in a medium with block structure," *Fiz.-Tekh. Probl. Razrab. Polezn. Iskop.*, No. 1, 14–21 (1988).
6. V. A. Saraikin, "The two-dimensional equations of motion for a block medium," in: *Proc. Conf. on Geodynamics and the Stress State of the Earth Interior* (Novosibirsk, October 4–7, 2005), Inst. of Mining, Sib. Div., Russian Academy of Sci., Novosibirsk (2006), pp. 200–207.
7. V. A. Saraikin, "Equations of motion for a block medium," in: D. D. Ivlev and N. F. Morozova (eds.), in: *Problems of Mechanics of Deformable Solids and Rock: Collected Papers Dedicated to the 75th Birthday of E. I. Shemyakin* [in Russian], Fizmatlit, Moscow (2006), pp. 652–658.
8. V. A. Saraikin, "Calculation of the waves propagating in a two-dimensional assembly of rectangular blocks," *Fiz.-Tekh. Probl. Razrab. Polezn. Iskop.*, No. 4, 32–42 (2008).
9. N. I. Aleksandrova "On the propagation of elastic waves in a block medium under pulsed loading," *Fiz.-Tekh. Probl. Razrab. Polezn. Iskop.*, No. 6, 38–47 (2003).
10. N. I. Aleksandrova and E. N. Sher, "Modelling of wave propagation in block media," *Fiz.-Tekh. Probl. Razrab. Polezn. Iskop.*, No. 6, 49–57 9(2004).